

## Pattern Formation in the NaOH + CuCl<sub>2</sub> Reaction

Péter Hantz\*

*Department of Theoretical Physics, Eötvös University, H-1117 Budapest, Pázmány sétány 1/A, Hungary, Department of Biochemistry, Eötvös University, H-1088 Budapest, Puskin utca 3, Hungary, and Department of Plant Taxonomy and Ecology, Eötvös University, H-1083 Budapest, Ludovika tér 2, Hungary*

*Received: July 19, 1999; In Final Form: January 7, 2000*

A simple chemical process with inorganic reactants (NaOH and CuCl<sub>2</sub>) is presented that leads to the formation of a great variety of spatial patterns previously observed only in much more complex systems. In particular, depending on the experimental conditions, Liesegang patterns and interacting chemical fronts may emerge. The latter can develop to form spirals and cardioids. At higher concentrations, unusual disordered patterns can build up, despite the striking simplicity of the experimental system. This type of pattern formation represents a new class of nonlinear chemical phenomena.

### Introduction

Pattern formations that are governed by reaction–diffusion processes are common in chemical and biological systems.<sup>1–5</sup> Some examples include the Liesegang banding,<sup>6–9</sup> cardioid and rotating spiral-shaped chemical waves in the Belousov–Zhabotinsky reactions,<sup>10–12</sup> and electrochemical waves in the chicken retina.<sup>13,14</sup> Furthermore, several sea shell patterns appear to be the result of pair production and mutual annihilation of traveling biochemical waves.<sup>15</sup> The simple chemical system presented in this paper can lead to the formation of the most important patterns that have been observed in the above systems.

### Experimental Section

Two series of experiments have been performed, for which the patterns were formed, either in gel sheets or in gel columns. The inner electrolyte CuCl<sub>2</sub> was distributed in a poly(vinyl alcohol) (PVA) gel, and the outer electrolyte NaOH was poured onto the top of the vertically placed gel and allowed to diffuse into it. The gel was made as follows: An 8.6 w/w % PVA solution was prepared by adding PVA powder (PVA 82 1038, Merck, AR) to high-purity water (supplied by a Labconco filter series) under continuous stirring at 70–80 °C. Complete solubilization was achieved by stirring the solution for 4 h at this temperature, and then it was allowed to cool to room temperature. The inner electrolytes of the required concentrations were obtained by adding different amounts of CuCl<sub>2</sub> (Reanal, AR) solutions to a series of PVA solutions, each of 100 mL volume. The acidity and cross linking of the gels were set by adding 1 mL of 1 M glutaraldehyde (Merck, AR) and 2 mL of 18.5 w/w % HCl (Reanal, AR) to the above mixtures. Finally, high-purity water was used to top off each solution to 200 mL. To prepare the experiments in gel sheets, the solutions were poured between pairs of glass plates to a height of 50 mm. The 83 × 102 mm glass plates were placed parallel to each other at a distance of 1.6 mm. For the experiments in gel columns, the solutions were poured into glass test tubes of 14 mm i.d. to a height of 100–120 mm.

Once the gelation took place (approximately 10 h), 3 and 6 mL of NaOH (Reanal, AR) outer electrolyte solutions of several concentrations were poured on the top of the vertically placed gel sheets and gel columns, respectively. The experiments were

carried out at room temperature. Photos of the gel sheets were taken by optical microscope, whereas those of the gel columns were taken with a scanner.

**Patterns in Gel Sheets.** First, the results are presented of the investigations when the reaction was taking place in a gel sheet, in which the concentrations of NaOH and CuCl<sub>2</sub> were  $a_0 = 8.0$  M and  $b_0 = 0.732$  M, respectively.

The simplest structures appear through the following sequence of events (Figure 1): The outer electrolyte, NaOH, diffuses into the gel containing the CuCl<sub>2</sub> inner electrolyte and a one-dimensional diffusion front is formed. Behind this front, a gel region is formed in which both of the reactants are present. This gel portion, where precipitation and pattern formation can occur, is referred to as the excitable region. Inside this excitable region there is a zone known as the reaction front, at which a primary precipitate is forming. This precipitate, assumed to be mainly Cu(OH)<sub>2</sub>, has blue color in reflected light and green color in transmitted light. The size of the primary precipitate seems to be between 0.01 and 0.4 μm because it looks homogeneous by investigations done with optical microscopy, but it is immobilized in the gel having a pore size of the order of 10 nm.

Later, the formation of the precipitate is halted at some points in the reaction front (Figure 1A). During the motion of the reaction front through the gel, these points expand into empty (precipitate-free) regions. Thus, the reaction front is split up into segments called reaction zones, each of them being limited by regressing edges. The empty regions are limited from above by two oblique, passive borders formed in the wake of the regressing edges (Figure 1B).

The angle of the passive borders, which limit the empty regions from the area where the precipitate has already formed, are determined by two perpendicular velocities: the speed of the diffusion front and that of the reaction zone's regressing edges. Between minutes 60 and 180 of the experiment, the order of magnitudes of both speeds were 0.1 mm/min. When the two regressing edges of such a reaction zone meet, a small cusp forms and the precipitation stops (Figures 1C and 2D). Note that at ~2 mm behind the region where the precipitate has already formed, the gel starts to shrink and no longer adheres to the glass plates. This effect, called syneresis, does not play an essential role in the pattern formation. Similar experiments

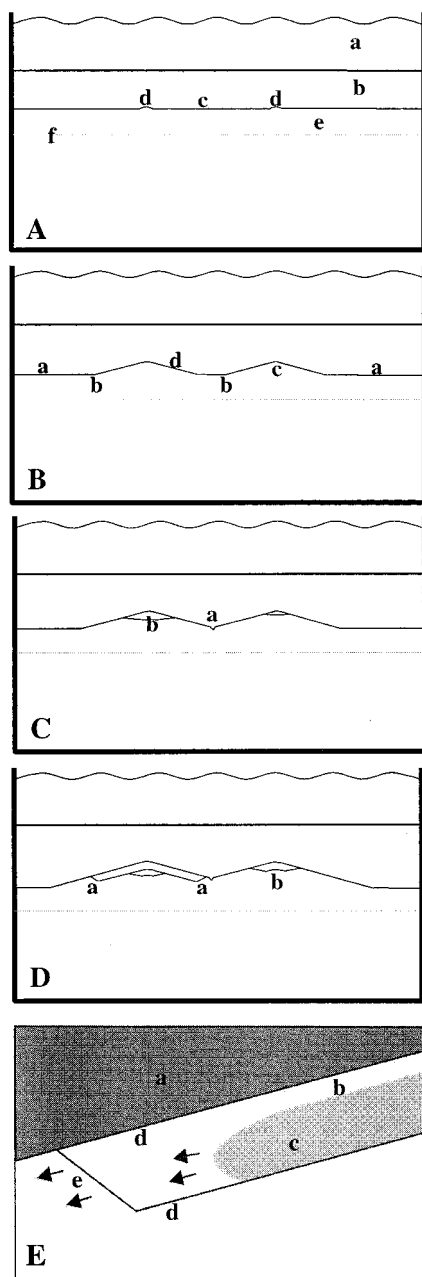


**Figure 1.** Main stages of pattern formation in gel sheets. (A) In some points of the reaction front, the formation of the precipitate is halted. The reaction front is split into reaction zones: (a) outer electrolyte; (b) primary precipitate; (c) reaction front; (d) points at which the formation of the precipitate is halted; (e) excitable region; and (f) approximate position of the diffusion front. (B) The points at which the formation of the precipitate is halted expand into empty regions: (a) reaction zones; (b) regressing edges; (c) empty (precipitate-free) region; and (d) passive edge. (It should be noted that the topmost empty regions usually form on bubbles located on the gel–outer electrolyte border). (C) Some time later, precipitation begins again at the top of the empty regions. The newly formed precipitate starts to fill the empty region: (a) encounter of two regressing edges and the formation of a small cusp and (b) new precipitate born in the empty region. (D) Pair production of reaction zones takes place when the reaction zone of the newly formed precipitate also splits: (a) new reaction zones formed by pair production and (b) pair production of reaction zones. (E) The process of the formation of the colloidal CuO precipitate (ripening): (a) Colloidal CuO (brown) precipitate in an elder pattern; (b) blind region that is never filled by the brown precipitate; (c) CuO formed in the primary precipitate generated by the reaction zone (e); (d) passive borders of the elder and younger precipitates; and (e) traveling reaction zone. The arrows show the progressing directions of the reaction zone and the invasion of the brown precipitate, respectively.

can be performed in agarose gel and thin liquid layers, respectively, in which syneresis does not occur but reaction fronts with similar dynamical properties emerge.

Some time later, the precipitate also emerges in the empty regions, beginning at the top of the regions (Figures 1C and 2A). Soon, the reaction zone of the younger precipitate formed in the empty region splits again. Thus, besides a new empty region, two new reaction zones are formed that propagate in the excitable region below the passive border of the preceding precipitate (Figures 1D and 2A). The precipitate, which was produced by these new reaction zones, is limited from above by the passive borders of the preceding precipitate and from below by the passive borders formed in the wake of the new regressing edges (Figures 1D,E, and 2A–E). At a later stage, the new reaction zones are no longer parallel with the diffusion front (Figures 1D and 2C). When approaching reaction zones meet, they annihilate each other, probably because of the depletion of the reactants in their surroundings. A small cusp forms at these annihilation points (Figure 2E).

In the next stage of the pattern formation, a ripening process starts in the primary blue-green precipitate, which then decays into a colloidal brown precipitate. According to the results of X-ray-scattering experiments, the brown precipitate is composed of CuO crystallites. The ripening process does not take place in a band of approximately 100  $\mu\text{m}$  thickness below the passive border of the preceding upper precipitate. Thus, between the regions filled with CuO, a thin band remains free of this precipitate at any time (Figures 1E and 2F). These blind bands are the dark oblique lines shown in Figure 2A,C–E.

Pair production and annihilation of traveling waves have been observed on several sea shell patterns. This behavior has been reproduced by mathematical models based on nonlinear reaction–diffusion equations.<sup>15</sup>

**Patterns in Gel Columns.** When the outer electrolyte (NaOH) is poured onto the top of a gel column, the diffusion front is expected to have the form of a disk, in contrast with the previous case, in which it has the shape of a thin line. In this case, the reaction zones involved in the pattern formation can perform a more complicated motion in the excitable region, leading to more complex patterns than in the previous case. A series of patterns were observed that depend on the outer and inner electrolyte concentrations.

**Liesegang Bands ( $a_0 = 0.5 \text{ M}$ ,  $b_0 = 0.0293 \text{ M}$ ).** Quasi-periodic precipitation in the wake of a moving reaction–diffusion front is called the Liesegang phenomenon. So far, three main classes of these patterns have been observed. The bandings are considered to be normal when the distance between consecutive bands increases with the band order, inverse when it decreases, and irregular when no regularity can be observed in the positions of the precipitate zones.<sup>7–9</sup>

In our experiments a green-colored substance is formed behind the diffusion front. This compound is optically more dense in separate, but randomly spaced regions along the gel column (Figure 3), and thus, it can be considered as an example of irregular Liesegang banding. The substance formed in this experiment does not seem to be a colloid because no particles are visible, even at 20  $\text{\AA}$  resolution using electron microscopy. In this case, syneresis of the gel has not been observed, and the ripening process leading to the brown precipitate mentioned above does not take place at all.

**Multiarmed Spirals ( $a_0 = 7.5 \text{ M}$ ,  $b_0 = 0.644 \text{ M}$ ).** At these concentrations, usually a trivial pattern (homogeneous precipitation) emerged only, if the outer electrolyte was simply layered on the gel column and allowed to diffuse into it. To obtain

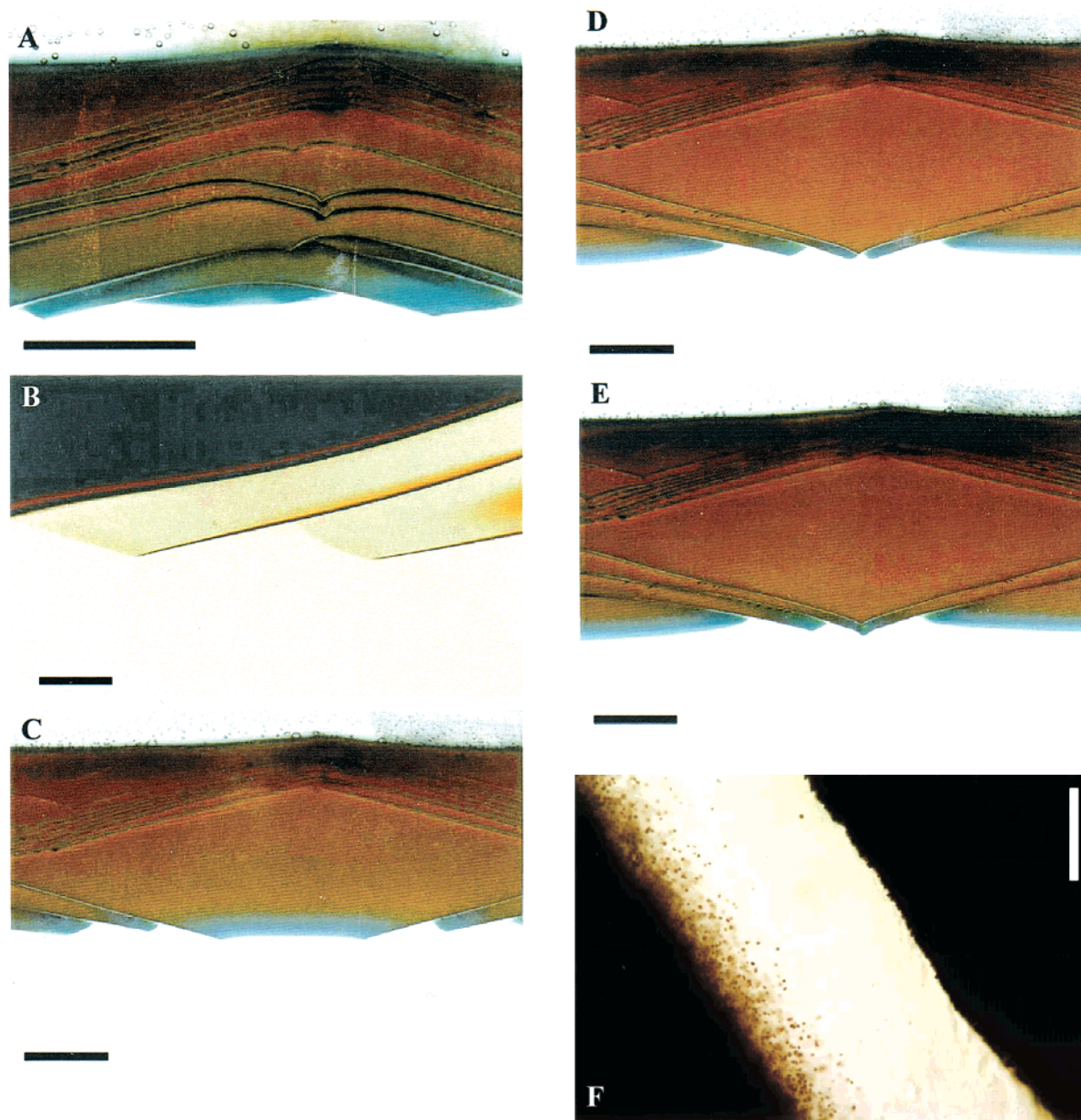


**Figure 2.** Patterns in gel sheets ( $a_0 = 8.0$  M,  $b_0 = 0.732$  M). Parts A, C, D, and E were taken using reflected light, whereas B and F were taken with transmitted light. (A) Precipitate begins to form at the top of an empty region. Note that the reaction zones on the two sides are no longer parallel with the diffusion front (scale bar = 0.25 cm). (B) Primary precipitate bands produced by propagating reaction zones: They are limited from above by the passive border of an elder precipitate and from below by the passive border formed in the wake of the regressing edge of the reaction zones. In this experiment, the gel sheet in which the pattern formation took place was 0.17 mm thick. (scale bar = 0.5 mm). (C–E) Three consecutive stages of the pattern development. Elapsed time from the beginning of the experiment is 97, 131, and 137 min, respectively (scale bar = 0.25 cm). (C) The reaction zone in the middle is getting smaller. (D) The regressing edges of the reaction zone in the center of the picture met, and therefore, the precipitation in this reaction zone stopped. Two small reaction zones can also be seen just before their annihilation. (E) The pattern after the annihilation of the reaction zones. (F) The colloidal CuO precipitate-free, blind band between an older (right) and a younger (left) precipitate (scale bar = 50  $\mu$ ).

nontrivial patterns, it was necessary to create special initial conditions, i.e., to increase the excitability at the top of the gel column. This was achieved by increasing the concentration of the inner electrolyte in a narrow top region by pouring 2.96 M CuCl<sub>2</sub> solution on the gel for 10 min. It is important to note that the increasing of the inner electrolyte's concentration at the top of the gel column is needed only to start the splitting of the reaction front because this process requires a higher degree of excitability than that for maintaining the reaction zones. Having removed the CuCl<sub>2</sub> solution, the outer electrolyte was poured on the gel. The reaction front split while passing through the gel region with increased inner electrolyte concentration, and the resulting reaction zones survived as they moved into

the part of the gel column where the inner electrolyte concentration was homogeneous and isotropic.

After a short transient, the reaction zones took the form of spiral arms, rotated around the axis of the gel column and moved down the gel as the diffusion front advanced (Figure 4A). Note that at first, the primary blue-green precipitate was formed in the wake of the reaction zones. Then, in a few minutes, it started to transform into the brown, colloidal CuO precipitate, except for a thin, blind region below the passive borders of the regions filled with precipitate by different reaction zones (Figure 4B,D).

In a central region, called the core, the reaction front did not split (Figure 4A,B). The diameter of the core is approximately 4 mm. Note that the diameter of the core is larger for the

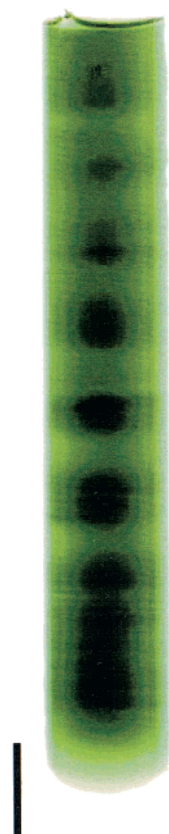


**Figure 3.** Irregular Liesegang pattern ( $a_0 = 0.5$  M,  $b_0 = 0.0293$  M; scale bar = 1 cm).

experiments in which the concentration of the inner electrolyte is slightly lower than the above value. Similar types of multiarmed spirals with well-defined cores have been observed in the experiments on the Belousov–Zhabotinsky reactions.<sup>11,16,17</sup>

The oblique motion of the spiral arm shaped reaction zones led to telescoped helicoid-like regions filled with colloidal CuO separated by the thin, blind areas (Figure 4C,D). The handedness of the helicoids present in a gel was determined by the random split and annihilation of the reaction zones at the upper end of the gel column. The pitch of the helicoids was constant during this experiment; i.e., the ratio of the reaction zone's horizontal and vertical velocities was constant (Figure 4C,D). Note that the latter is determined by the velocity of the diffusion front, which decreases in time.

**Cardioid-Like Patterns ( $a_0 = 8.0$  M,  $b_0 = 0.732$  M).** At these concentrations, the types of patterns formed were unpredictable: in 70% of the experiments, rotating reaction zones were formed similar to the spiral arms presented above, and in 30% of the cases, cardioid-shaped patterns emerged. The development of the latter passed through various stages as the diffusion front moved through the gel column (Figure 5A,B). At a certain point in the central part of the reaction front, a small, arch-shaped split occurred, in which precipitation did not take place. The external border of the arch was a regressing edge, leaving behind an empty area that subsequently filled with precipitate. In the next stage of the development, the arch grew, and its ends turned against each other. When they met, the pattern took the form of a closed cardioid (Figure 5A). At that moment, the reaction front was split into two parts. As the diffusion front advanced, the outer reaction zone, which had a cardioid-shaped regressing edge, was getting smaller, whereas the inner one was filling the empty region left by the outer zone

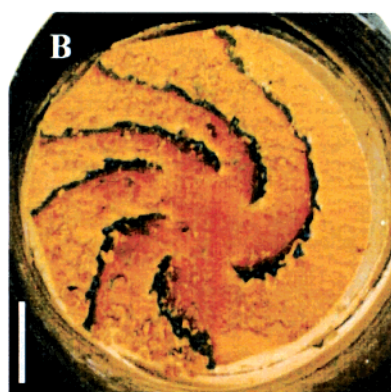
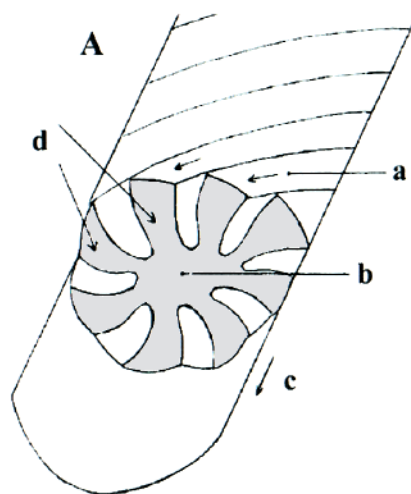


**Figure 4.** Patterns formed in a gel column by reaction zones shaped like spiral arms ( $a_0 = 7.5$  M,  $b_0 = 0.644$  M). (A) The structure of the reaction zones: (a) growing direction of the reaction zones; (b) core; (c) advancing direction of the diffusion front; and (d) reaction zones (B). Cross section of the gel column after the reaction took place. The black curves are the traces of the blind, empty areas. In the central region (core), no front split took place (scale bar = 0.25 cm). (C–D) The gel column and its longitudinal section after the reaction took place. The “plastic” form is caused by the syneresis of the gel (scale bar = 1 cm).

with precipitate. When the diameter of the cardioid reached  $\sim 6$  mm, a new split occurred in the inner reaction zone (Figure 5B).

A few minutes after the reaction zones produced the blue-green precipitate, the ripening process began to generate the

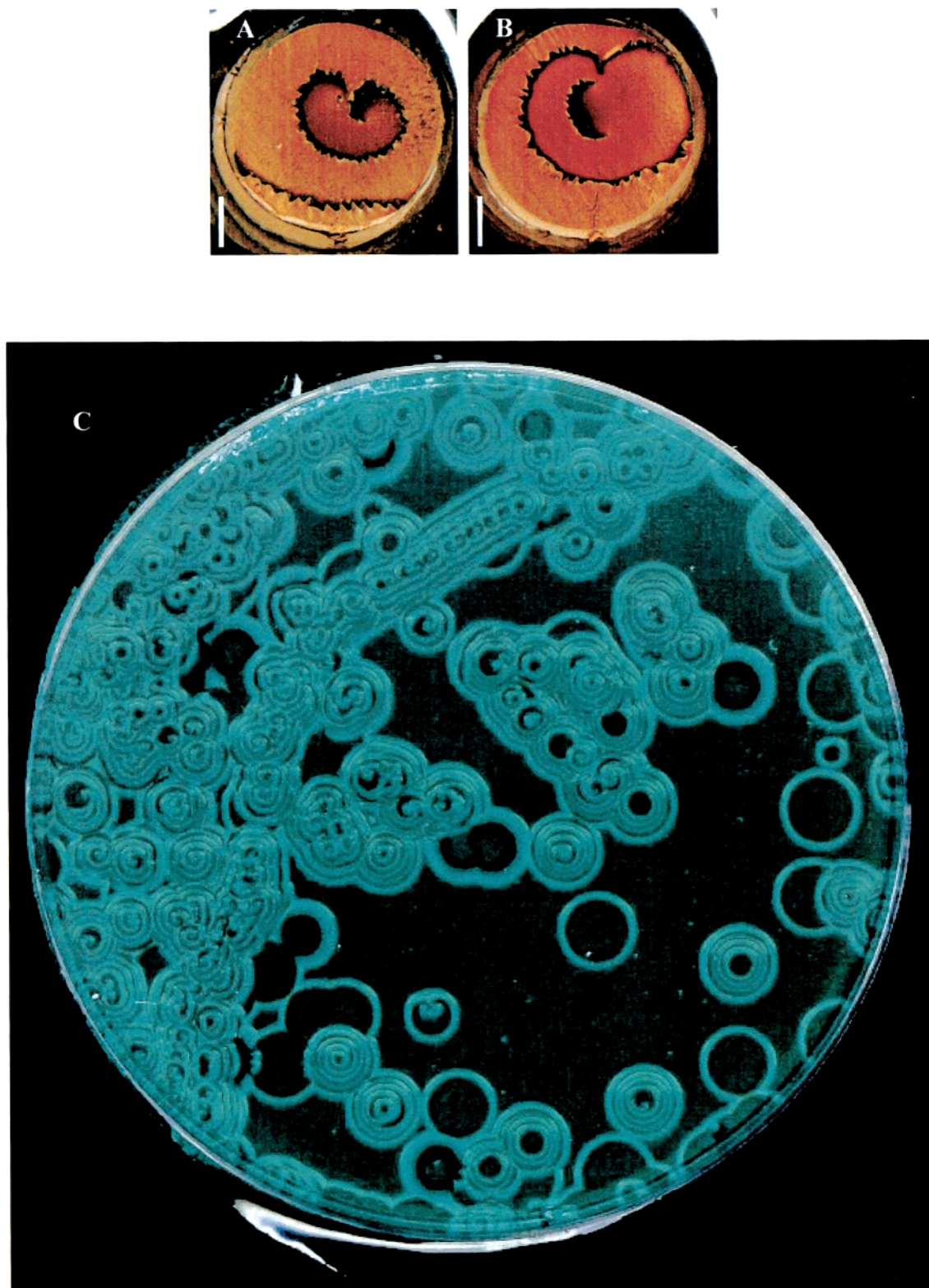


**Figure 5.** (A–B) Cardioid-like patterns in a gel column ( $a_0 = 8.0$  M,  $b_0 = 0.732$  M). Two cross sections of the gel column after the reaction took place, representing consecutive stages of the pattern development. Enlargement of the elder and birth of the younger, blind band (dark curve) can be observed (scale bar = 0.25 cm). (C) Patterns in gel placed in a Petri dish of 8.7 cm inner diameter. Cardioid and spiral-shaped patterns can also be observed. The dish was put on the scanner while the reactions were going on, and the picture was taken from below. The light curves are the passive borders of the precipitates produced by the consecutive reaction zones.

brown precipitate. Only the thin, blind bands below the passive borders of the regions precipitated by different reaction zones remained empty of the brown precipitate. Note that spiral and cardioid-shaped patterns are not the result of border effects

caused by the test tubes. Similar patterns also appeared in experiments performed in gels having much larger diameters (Figure 5C).

It is remarkable that the evolution of the cardioid-shaped

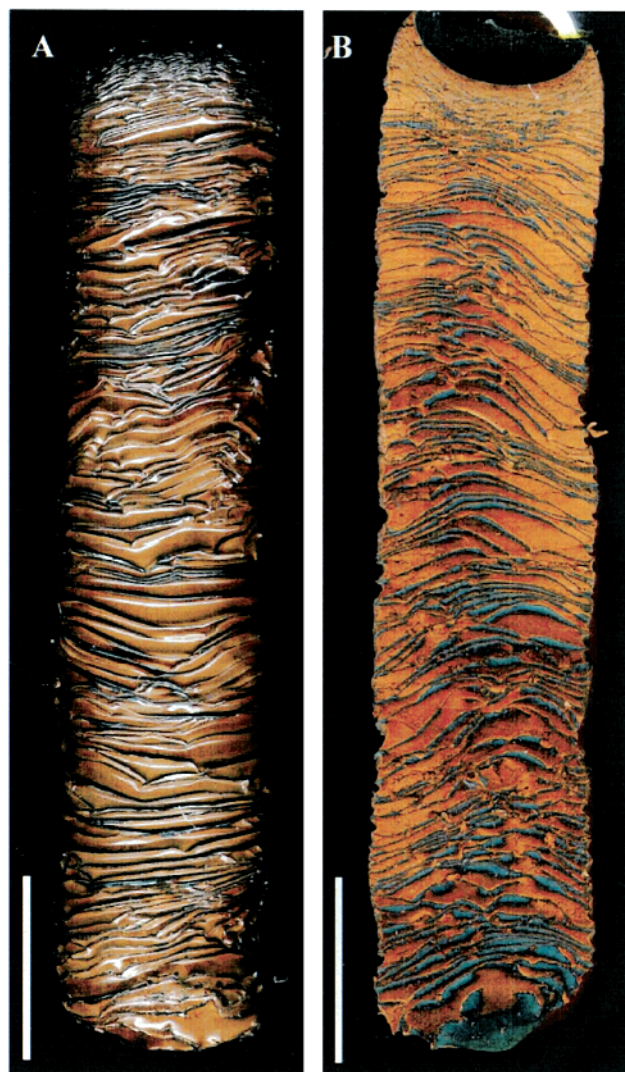


**Figure 6.** Disordered patterns formed in a gel column. The electrolyte concentrations were very high ( $a_0 = 15.0$  M,  $b_0 = 0.879$  M). Scale bar = 1 cm. (A) The gel column after the reaction took place. (B) Longitudinal section of the gel column. Frequent birth and annihilation of reaction zones can be observed.

electrochemical waves detected in chicken retina goes through approximately the same developmental stages as those mentioned above.<sup>13,14</sup>

**Irregular, “Cabbage-Like” Patterns ( $a_0 = 15$  M,  $b_0 = 0.879$  M).** At these high concentrations, regular, ordered patterns no longer formed. The traveling reaction zones were very close to each other; they frequently met and annihilated. At the same time, splitting of the reaction zones was very frequent. All these phenomena resulted in the pattern shown in Figure 6A,B.

The conditions for obtaining the above-mentioned patterns in gel columns are summarized in Figure 7. Note that the most relevant patterns are located near the diagonal of the diagram. For the experiments using gel sheets, this variety of patterns did not appear.

## Discussion

No detailed theoretical explanation for these structures has been found. Each of these patterns has been observed in various reaction systems, but no other system is known that produces all of these phenomena. Also, traveling waves and spiral patterns have been produced by mechanistically very complicated

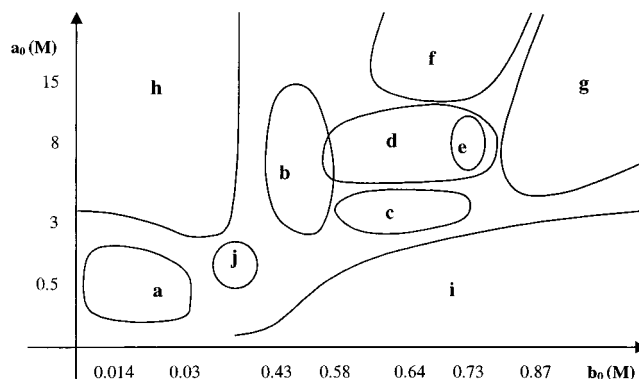


**Figure 7.** Concentration space of the reagents for the patterns formed in gel columns: (a) irregular Liesegang banding; (b) homogeneous brown precipitate; (c) distorted helicoidal patterns; (d) helicoidal patterns; (e) cardioid patterns; (f) random helicoidal patterns; (g) cabbage-like patterns; (h) homogeneous green or purple precipitate; (i) the precipitation stops near the top of the gel column because of the depletion of the outer electrolyte; and (j) other types of quasiperiodic patterns.

chemical systems, but no other simple inorganic reaction is known to produce such a wide variety of spatial formations.

Some of the main characteristics of the patterns formed in the gel sheets can be explained by assuming that a diffusive substance is formed along the reaction zones, and a critical concentration of this intermediate (not yet determined) is needed for the formation of the blue-green precipitate. If we suppose that this substance is produced only by the reaction zones (and not also by the passive borders), then its concentration decreases around the regressing edges. Thus, the formation of the blue-green primary precipitate is forced to regress in the direction along the reaction zone. Note that the reaction takes place in nonexcitable media, but as the diffusion front advances, the reaction zones penetrate in new, excitable gel regions. This supposition also explains why the precipitation stops when two regressing edges of a reaction zone meet: at the meeting point, the concentration of the intermediate becomes so low that no precipitation can occur. The annihilation of traveling reaction zones moving toward each other can be explained by supposing that the electrolytes are depleted from the surroundings of the meeting point during the formation of the intermediate. Colloidal growth processes,<sup>18,19</sup> which take place in the wake of the reaction zones, are relevant only in the second stage of the pattern formation, i.e., the birth of the brown precipitate.

The chemical instability arising from differential transport of heat and matter is known to produce temperature and concentration waves<sup>20</sup> and may contribute to the pattern formation. Although the thermochemistry of the processes is not known, it is assumed that thermal effects do not contribute significantly to the pattern formation. Precipitation after the first experimental hour is very slow, and therefore, local temperature changes in the reaction front are probably insignificant. Note that the results are quite temperature-insensitive: the patterns observed in gel columns at room temperature are also forming at 10 and 55 °C, too.

The phenomena presented in this article are not specific to a single chemical system. Slightly different patterns form when other copper or silver salts (e.g., Cu(NO<sub>3</sub>)<sub>2</sub> and AgNO<sub>3</sub>) are used instead of CuCl<sub>2</sub>, or the reaction proceeds in PVA solution without gelation, and even in thin electrolyte layers. Also, a rich variety of patterns emerge when agarose gel is used instead of PVA.

**Acknowledgment.** I am indebted to L. Szilágyi, Z. Rácz, T. Turányi, Z. Noszticziusz, E. Kőrös, M. Orbán, E. Szathmáry, and E. Keszei for useful discussions; D. Sherrington (University of Oxford), M. Zrínyi (Budapest University of Technology), I. Oláh, M. Palkovits, and A. Magyar (Semmelweis University Medical School, Budapest) for the opportunity to work at their departments; Gy. Faigel, G. Zboray, G. Bortel, J. Kovács, and A. Reichard for their help in some experiments. I acknowledge the support of Gy. Kéri, L. Gráf, K. Tóth, A. Málnási, and I. Jalsovszky. Also, I am thankful for the financial assistance of the Ösztöndíj Foundation, of the Orbán Balázs Foundation, of the Hungarian Ministry of Education, and of the Hungarian Research Funds (Grant No. OTKA T029792). Additional experimental details are available from the author on request (hantz@poe.elte.hu or hantz@ludens.elte.hu).

### References and Notes

- (1) Krinsky, V. I., Ed. *Autowaves and Structures Far from Equilibrium*; Springer Series in Synergetics; Springer: Berlin, 1984.
- (2) Murray, J. A. *Mathematical Biology*; Springer: Berlin, 1993.
- (3) Cross, M. C.; Hohenberg, P. C. *Rev. Mod. Phys.* **1993**, *65*, 851.
- (4) Koch, J. A.; Meinhardt, H. *Rev. Mod. Phys.* **1994**, *66*, 1481.
- (5) Scott, S. *Oscillations, Waves and Chaos in Chemical Kinetics*; Oxford University Press: Oxford, 1995.
- (6) Liesegang, R. E. *Naturwiss. Wochenschr.* **1896**, *11*, 353.
- (7) Henish, H. *Crystals in Gels and Liesegang Rings*; Cambridge University Press: Cambridge, 1988.
- (8) Schibechi, R. A.; Carlsen, C. *J. Chem. Educ.* **1988**, *65*, 365.
- (9) Antal, T.; Droz, M.; Magnin, J.; Rácz, Z.; Zrínyi, M. *J. Chem. Phys.* **1998**, *109*, 9479.
- (10) Field, J., Burger, M., Eds. *Oscillations and Travelling Waves in Chemical Systems*; Wiley: New York, 1985.
- (11) Agladze, K. I.; Krinsky, V. I. *Nature* **1982**, *296*, 424.
- (12) Schütze, J.; Steinbeck, O.; Müller, S. C. *Nature* **1992**, *356*, 45.
- (13) Gorelova, N. A.; Bures, J. *J. Neurobiol.* **1983**, *14*, 353.
- (14) Winfree, A. T. *When Time Breaks Down: Three-Dimensional Dynamics of Electrochemical Waves and Cardiac Arrhythmias*; Princeton University Press: Princeton, 1987.
- (15) Meinhardt, H. *The Algorithmic Beauty of Sea Shells*; Springer: Berlin, 1995.
- (16) Nagy-Ungvárai, Zs.; Ungvárai, J.; Müller, S. C. *Chaos* **1992**, *3*, 15.
- (17) Müller, S.; Plessner, T.; Hess, B. *Science* **1985**, *230*, 661.
- (18) Hunter, R. J. *Introduction to Modern Colloid Science*; Oxford University Press: Oxford, 1993.
- (19) Gránásy, L. *Diffus. Defect Data, Pt. B (Solid State Phenomena)* **1997**, *56*, 67.
- (20) Yakhnin, V. Z.; Rovinsky, A. B.; Menzinger, M. *J. Phys. Chem.* **1994**, *98*, 2116.